Segregation and Phase Transformations Along Superlattice Intrinsic Stacking Faults in Ni-based Superalloys

T.M. Smith[1,*], B. D. Esser[2], B. Good[1], M.S. Hooshmand[2], G.B. Viswanathan[2], C.M.F. Rae[3], M. Ghazisaeidi[2], D. W. McComb[2], M.J. Mills[2]

[1] NASA Glenn Research Center, 21000 Brookpark Rd. Cleveland OH 44135, USA
[2] Center for Electron Microscopy and Analysis, The Ohio State University, Columbus OH 43212, USA
[3]Department of Materials Science and Metallurgy, University of Cambridge, Cambridge CB2 3QZ, UK

Support provided by NASA's Aeronautics Research Mission Directorate (ARMD) – Convergent Aeronautics Solutions Project and NASA's Advanced Air Transport Technology (AATT) Project Office (ARMD) *and NSF DMREF Program*

THE OHIO STATE UNIVERSITY

UNIVERSITY OF CAMBRIDGE

Ni-Based Superalloys for Turbine Disks

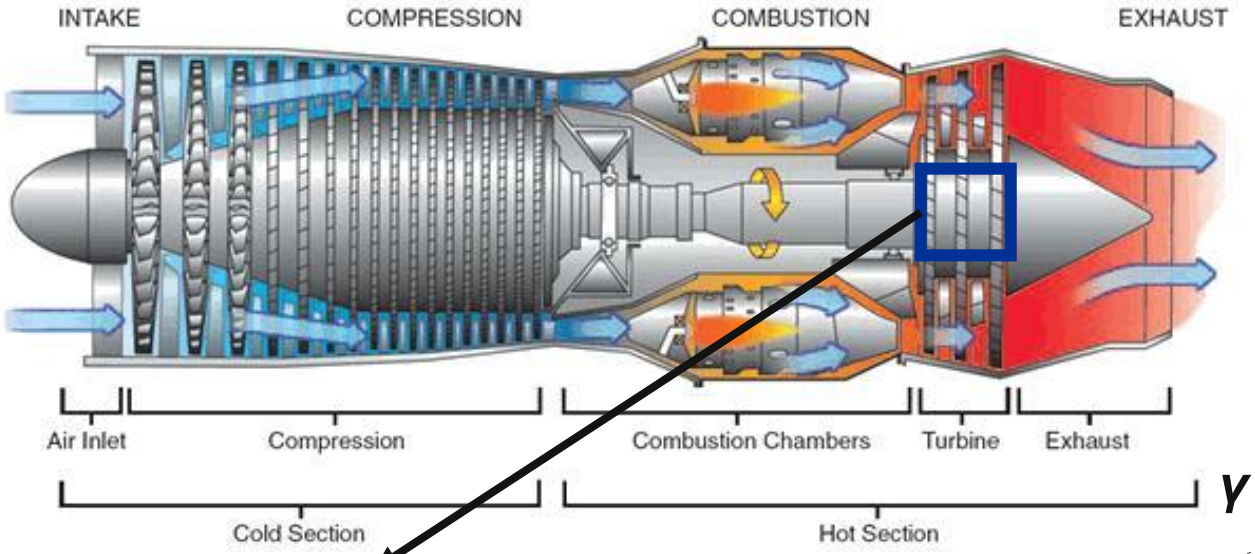

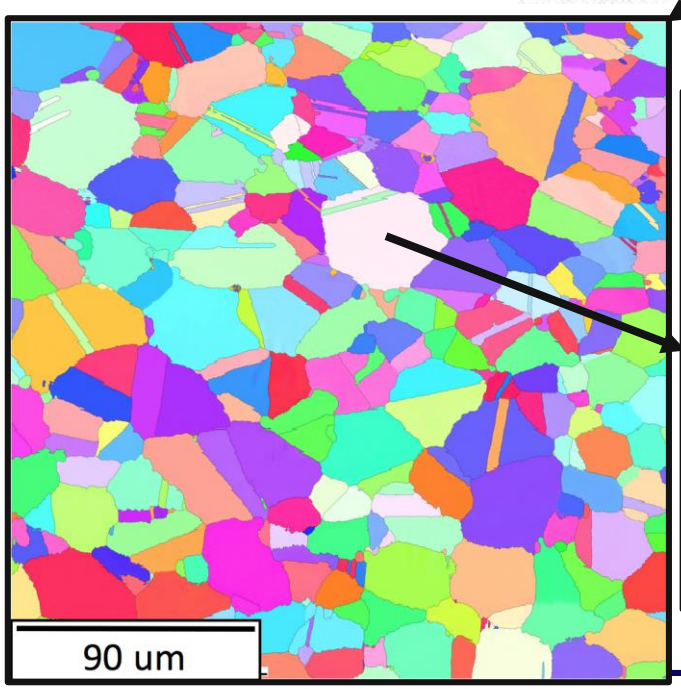

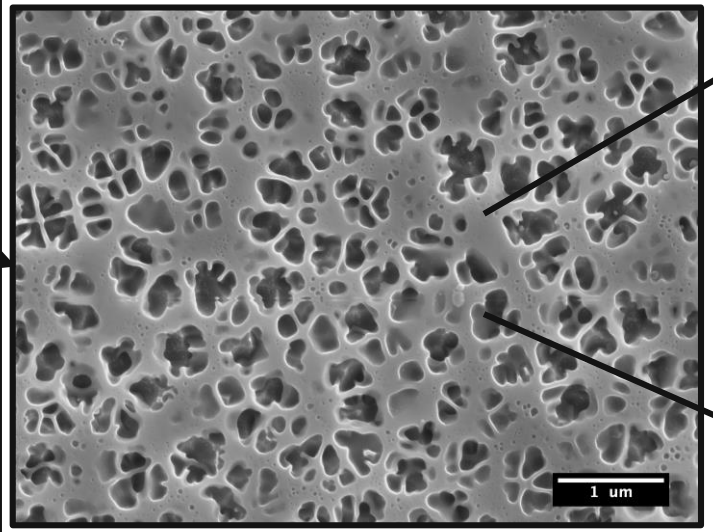

γ Phase (FCC)

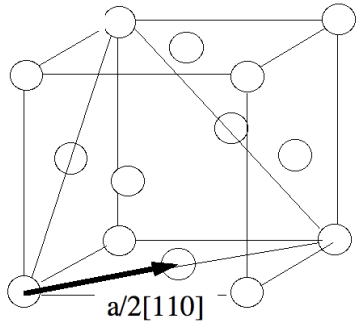

γ' Phase ($L1_2$)

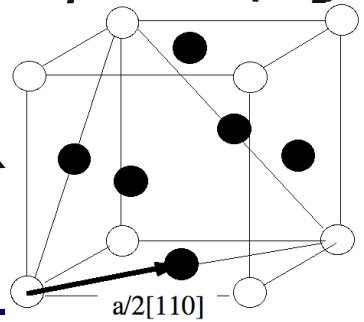

Motivation for Mechanistic Studies

- Material advancements are required to accommodate the higher compressor exit temperatures in jet turbine engines (>700°C near the rotor rim) for improved efficiency and pollution reduction.

- New deformation mechanisms will become dominant at these higher operating temperatures along with a need for improved creep properties in these disk alloys.

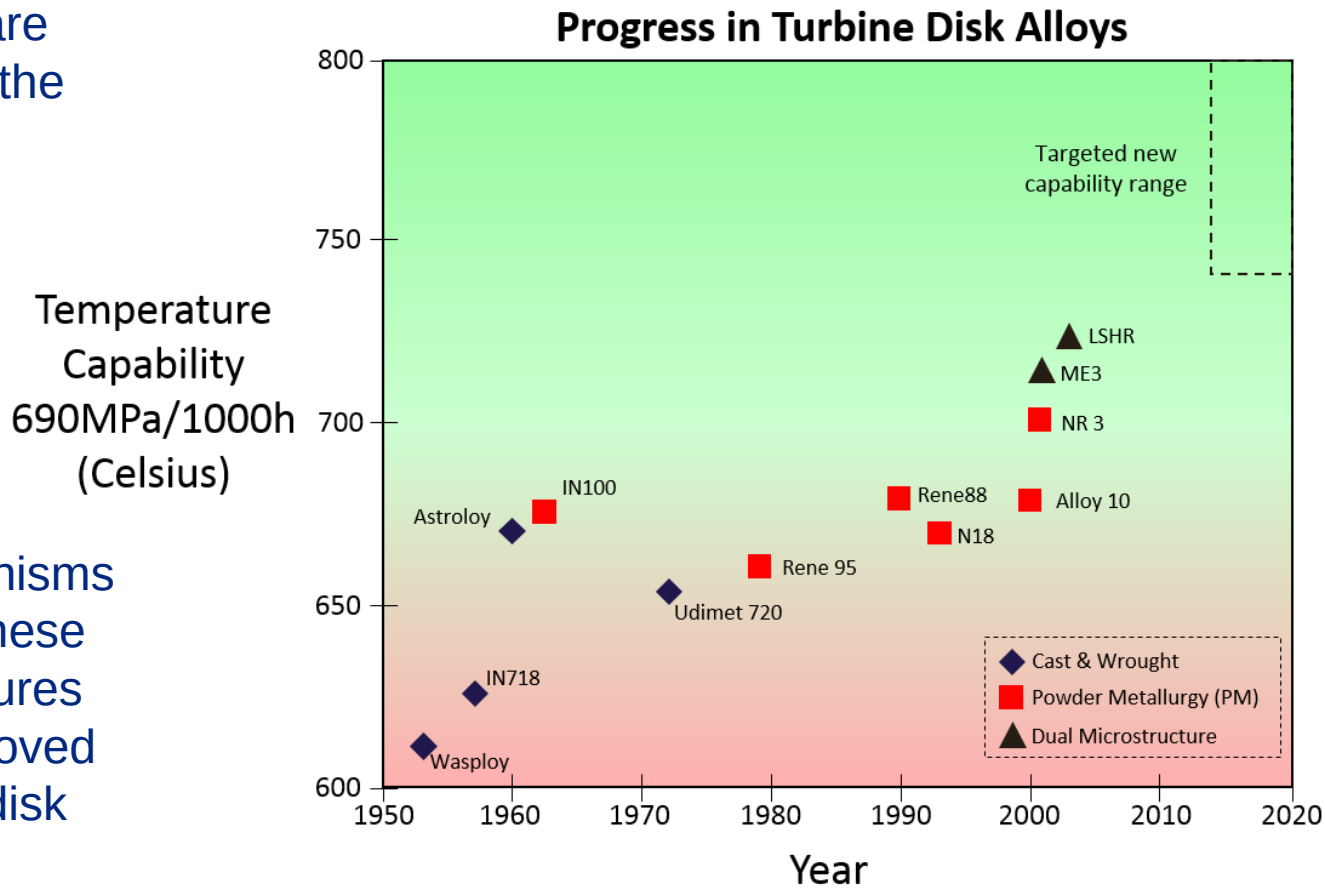

Deformation Mechanisms in Superalloys

Disk Alloys

T<700° C

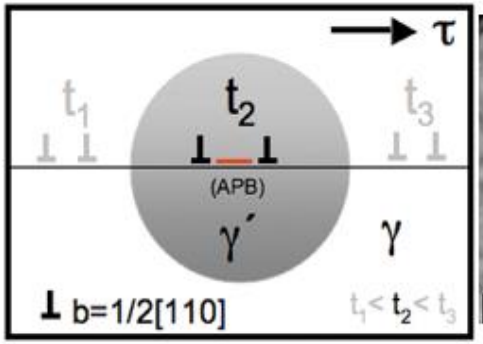

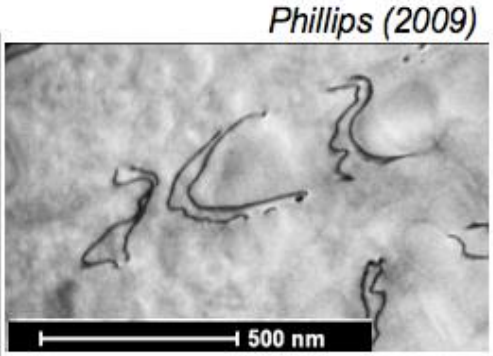

Phillips (2009)

Athermal γ' shearing by 1/2<110> dislocations

γ Phase (FCC)

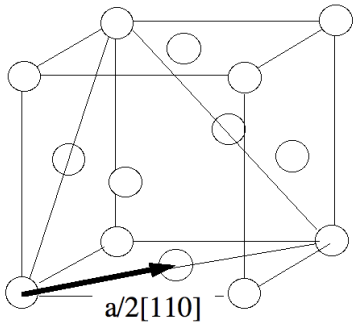

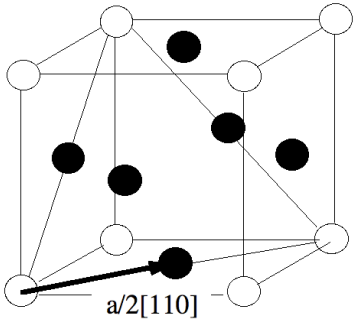

γ' Phase ($L1_2$)

Blade Alloys

T>900° C

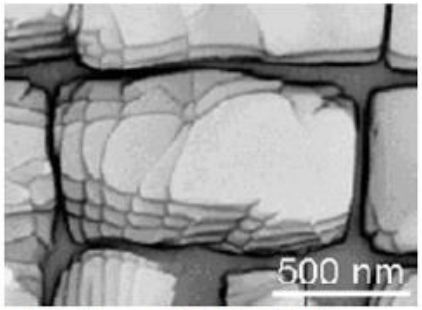

Epishin and Link (2008)

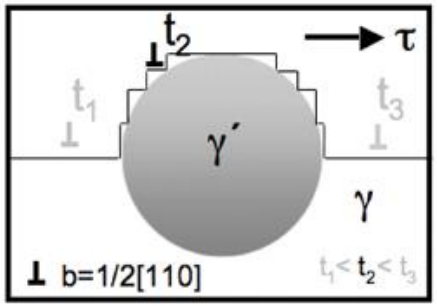

Climb By-Pass of γ′ by individual 1/2<110> dislocations

Deformation Mechanisms in Superalloys

Disk Alloys

T<700° C

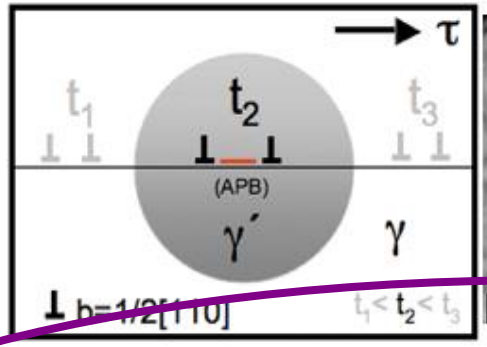

Phillips (2009)

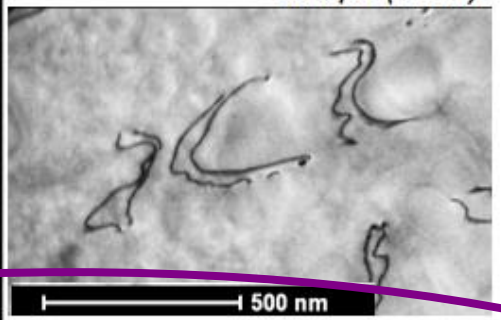

Athermal γ' shearing by 1/2<110> dislocations

Novel mechanisms:

- **Stacking Fault Cutting**
- **Microtwinning**
- **Stacking Fault Ribbons**

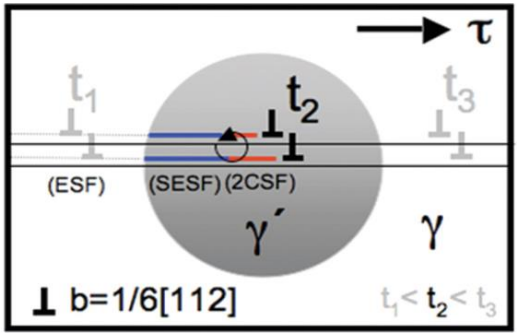

Diffusion mediated creep deformation

Blade Alloys

T>900° C

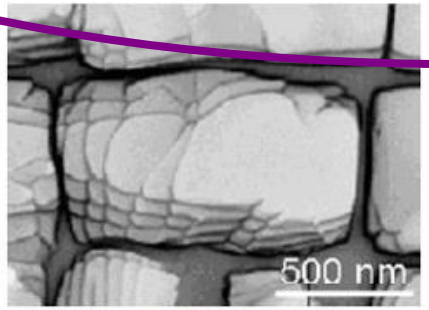

Epishin and Link (2008)

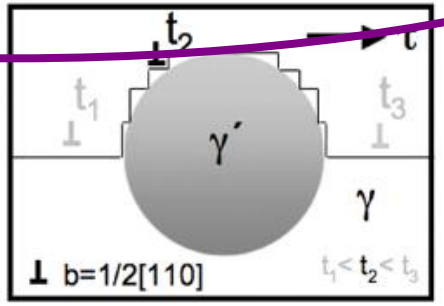

Climb By-Pass of γ′ by individual 1/2<110> dislocations

Deformation Mechanisms: Microtwinning

SESFs

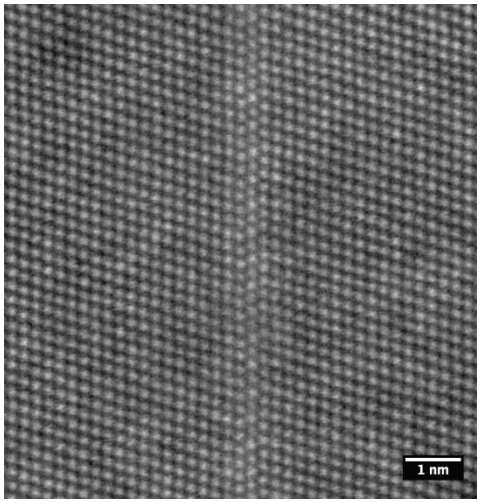

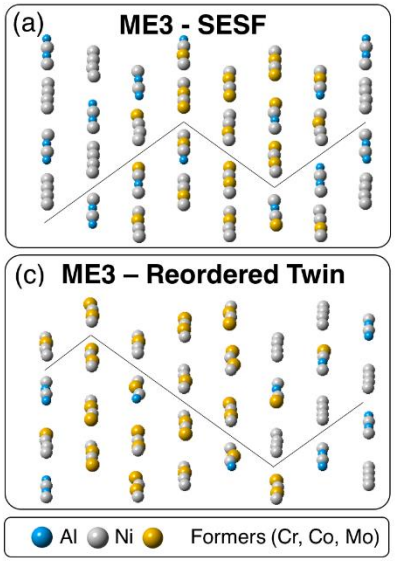

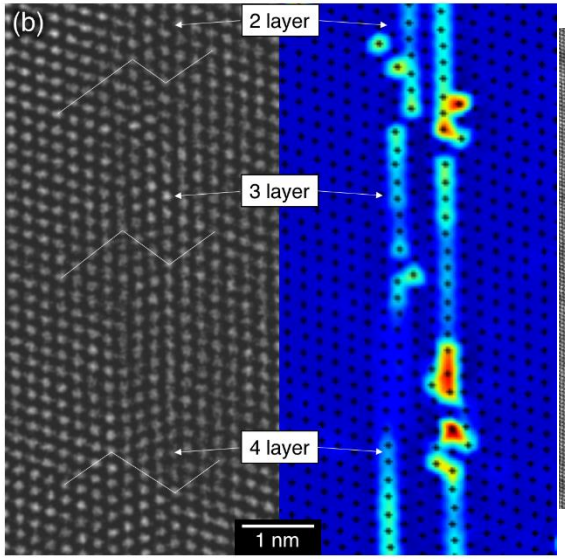

Microtwins

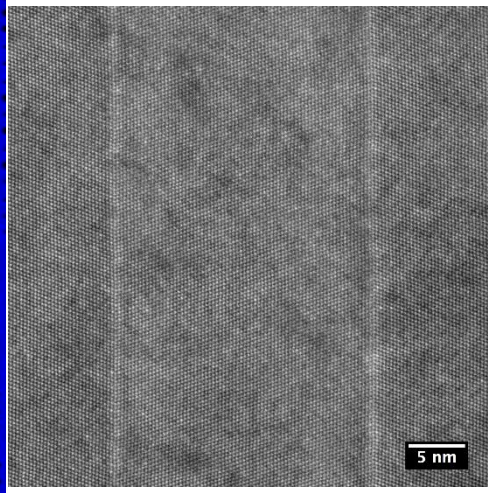

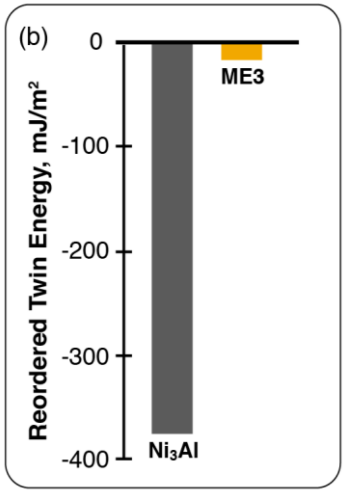

- Microtwins thicken from SESFs via additional Shockley partial pairs shearing along (111) fault planes
- Segregation of “γ former” elements strongly reduces energy penalty for twinning

Deformation Mechanisms: Microtwinning

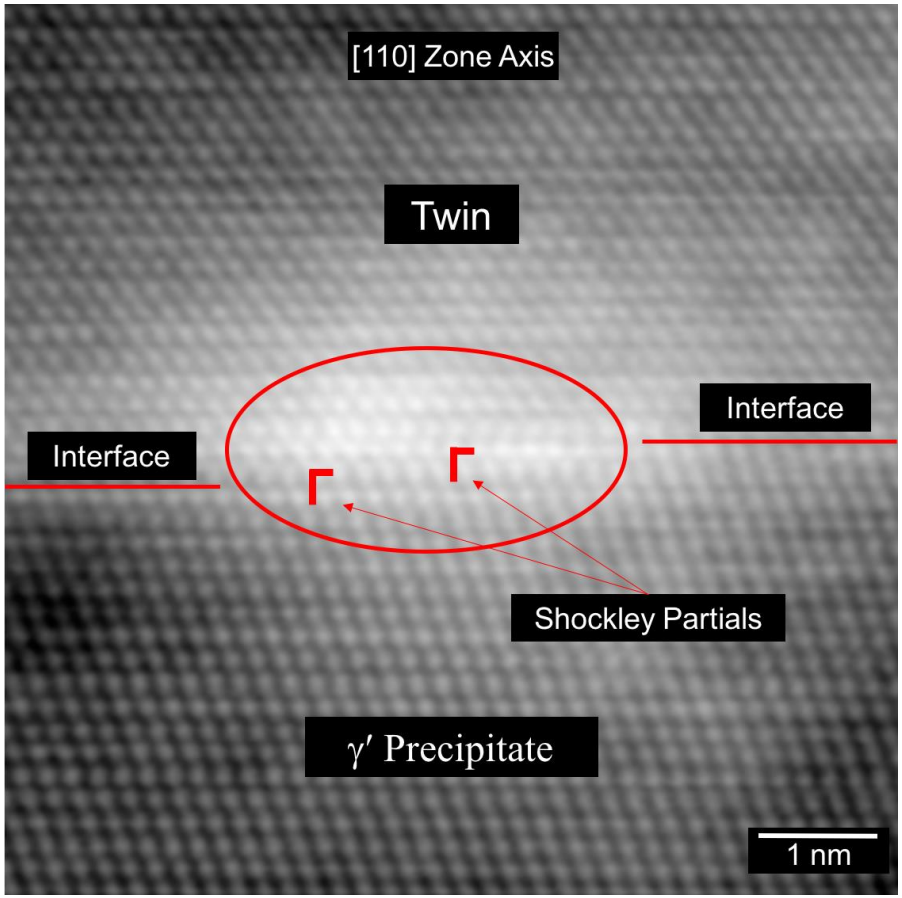

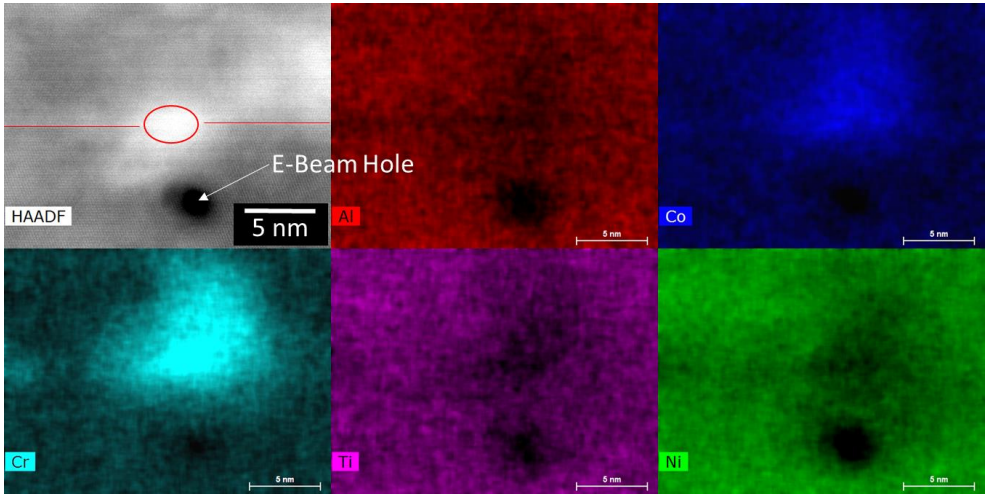

- Dissimilar matrix dislocations react at γ/γ' interface – shearing by Shockley partial pairs
- Stacking fault shearing controlled by segregation and Cottrell atmospheres
- Rate of microtwinning also limited by segregation and Cottrell atmospheres
- Can these deformation modes be mitigated/eliminated?

Smith, et al. Acta Materialia, 2017

Deformation Mechanisms: Microtwinning

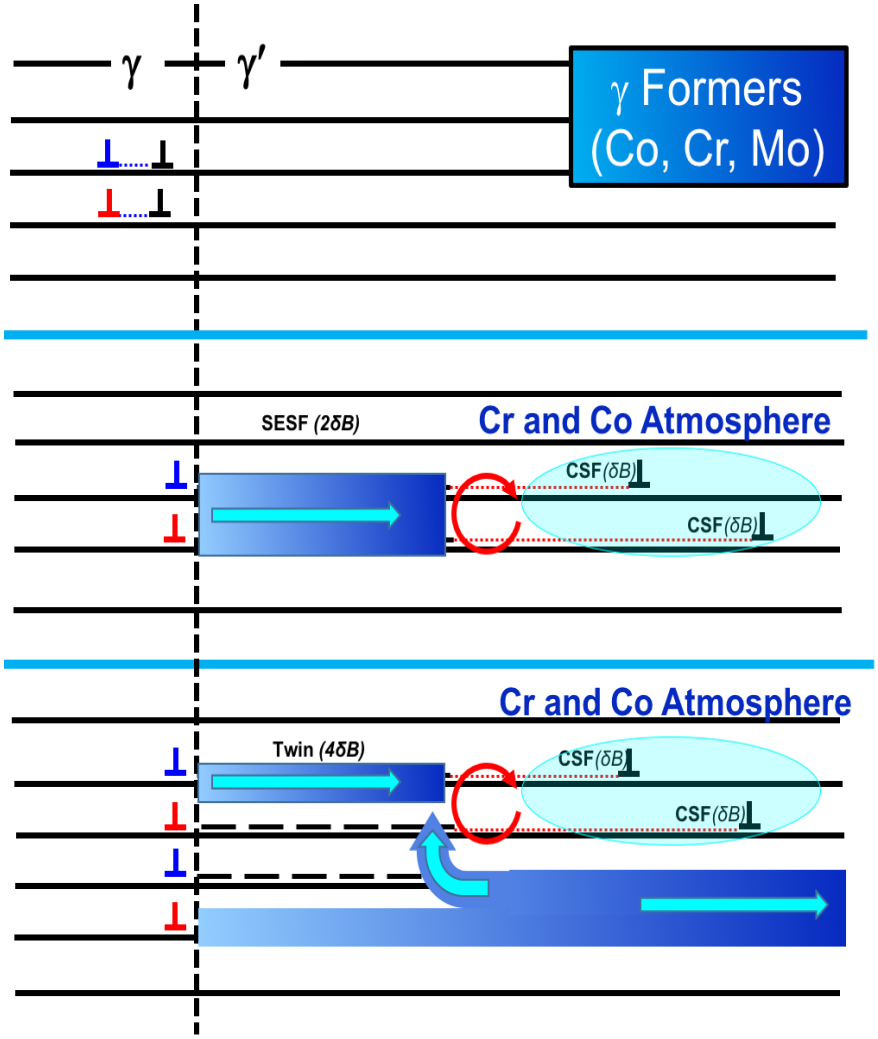

Smith, et al. Acta Materialia, 2017

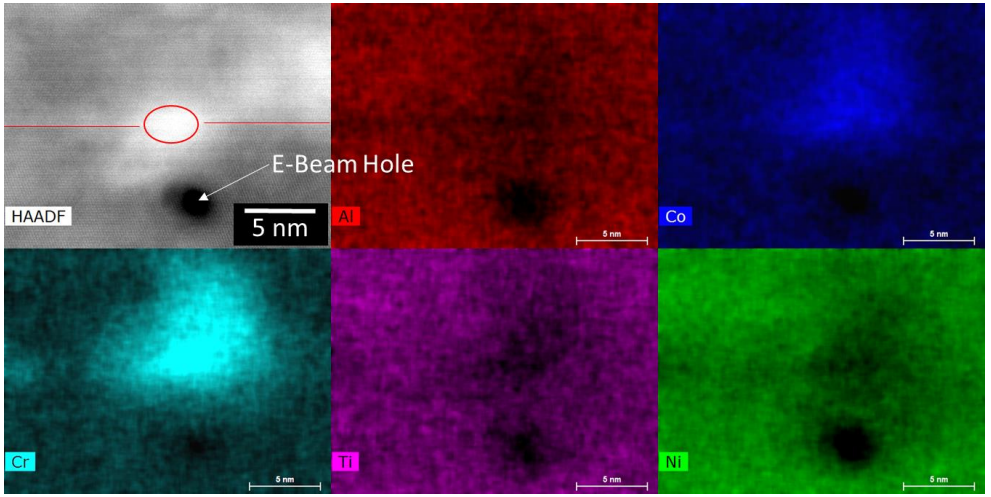

- Dissimilar matrix dislocations react at γ/γ' interface – shearing by Shockley partial pairs
- Stacking fault shearing controlled by segregation and Cottrell atmospheres
- Rate of microtwinning also limited by segregation and Cottrell atmospheres
- Can these deformation modes be mitigated/eliminated?

Phase Transformation Strengthening

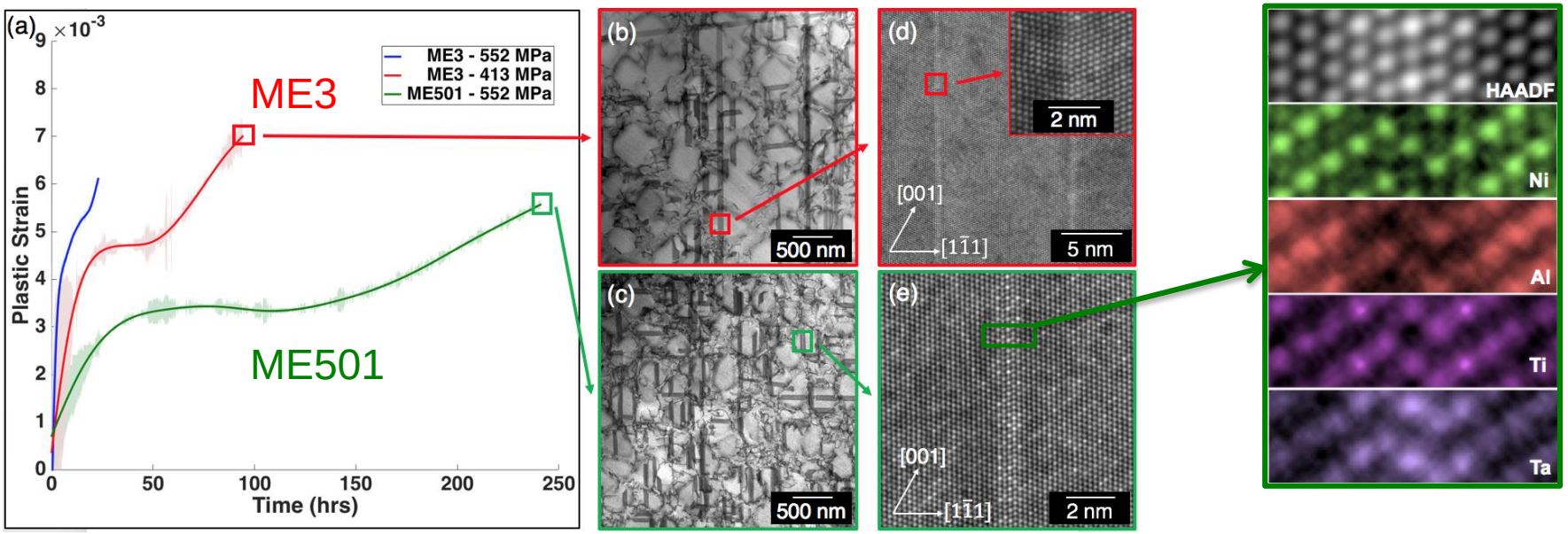

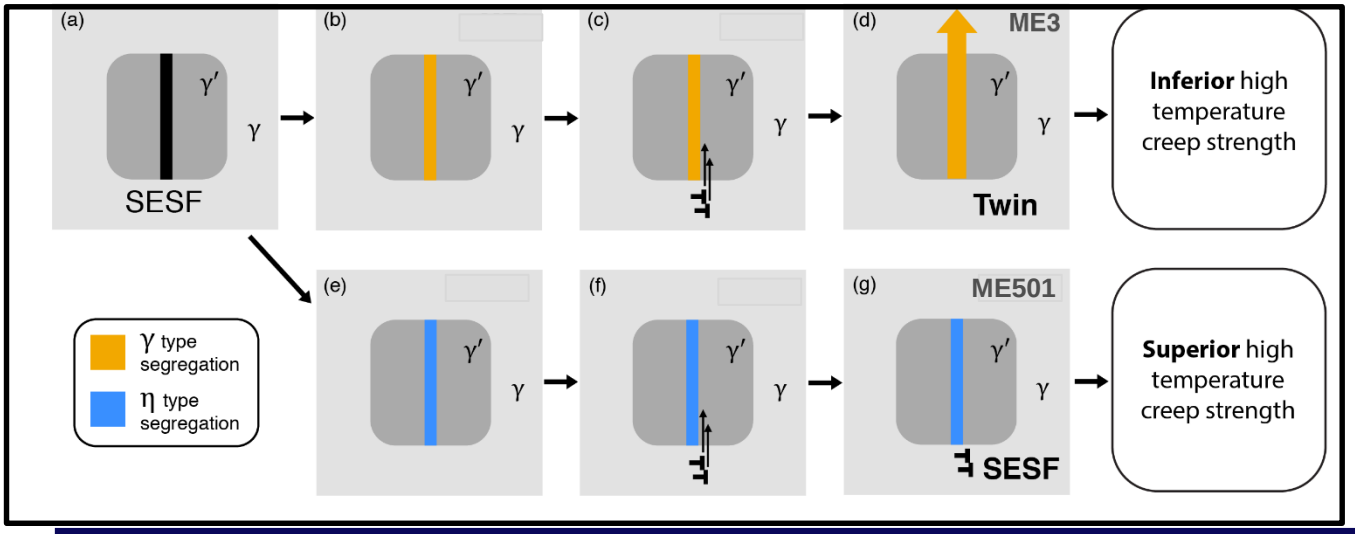

New insight into alloy effects:

- Segregation of γ formers in ME3 promotes microtwinning
- Formation of η phase at faults in ME501 inhibits microtwinning and improves creep strength

Smith, et al. Nature Communications, 2016

What diffusion mechanisms are present during SISF formation?

Local phase transformations in Ni-base superalloys

Stress: 414-552MPa
Temperature: 760°C

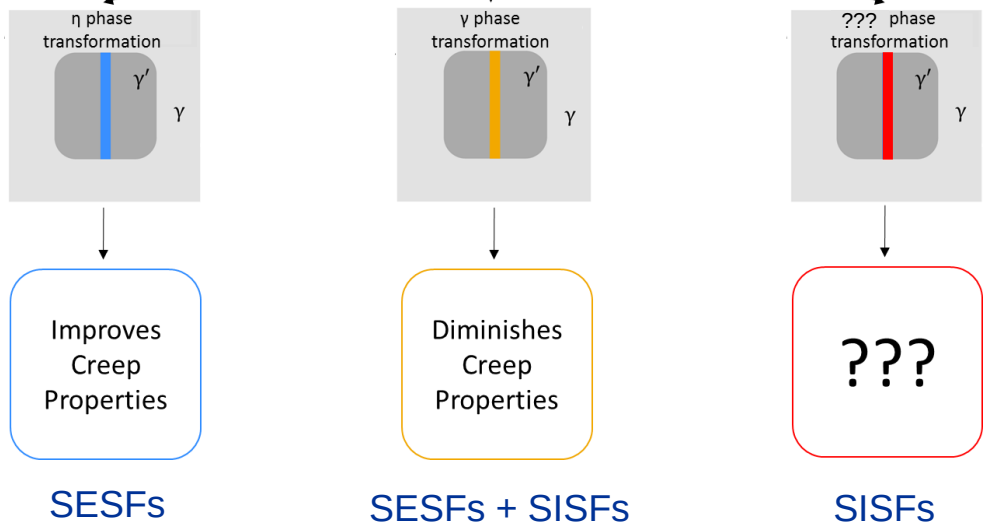

Is there a phase transformation along SISFs that can be promoted over the detrimental γ phase?

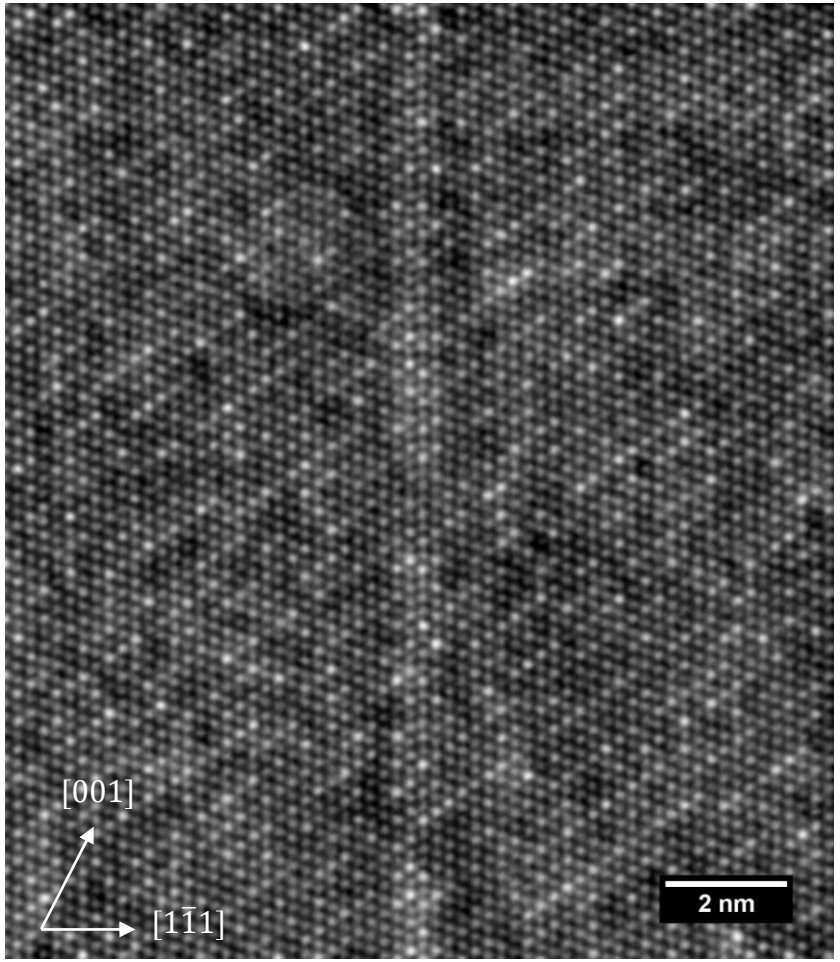

CMSX-4

Material Preparation

Alloy	Ni	Cr	Co	Mo	W	Nb	Ta	Al	Ti	Hf	Re	Zr	B	C
ME501	Bal.	12	18	2.9	3	1.5	4.8	3	3	0.4	0	0.05	0.03	0.05
CMSX-4	Bal.	6.5	9.6	0.6	6.4	0	6.5	5.6	1	0.1	3	0	0	0

ME501: [001] compression creep test was performed at 760°C under a stress of 552MPa to a plastic strain of 0.5%.[1]

CMSX-4: [001] tensile creep test was performed at 750°C under a stress of 750MPa to a plastic strain of 8.6%.[2]

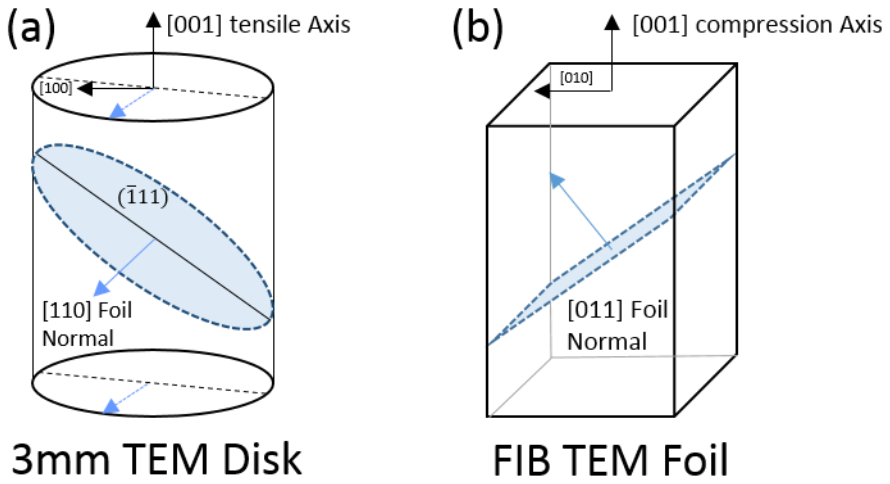

[1]T.M. Smith, B. Esser, N. Antolin, G. Viswanathan, T. Hanlon, A. Wessman, D. Mourer, W. Windl, D. McComb, M. Mills. *Acta Mater.*, 2015, vol. 100, pp. 19-31

[2]V.A. Vorontsov, L. Kovarik, M.J. Mills, and C.M.F. Rae: *Acta Mater.*, 2012, vol. 60, pp. 4866–78.

SISF Formation

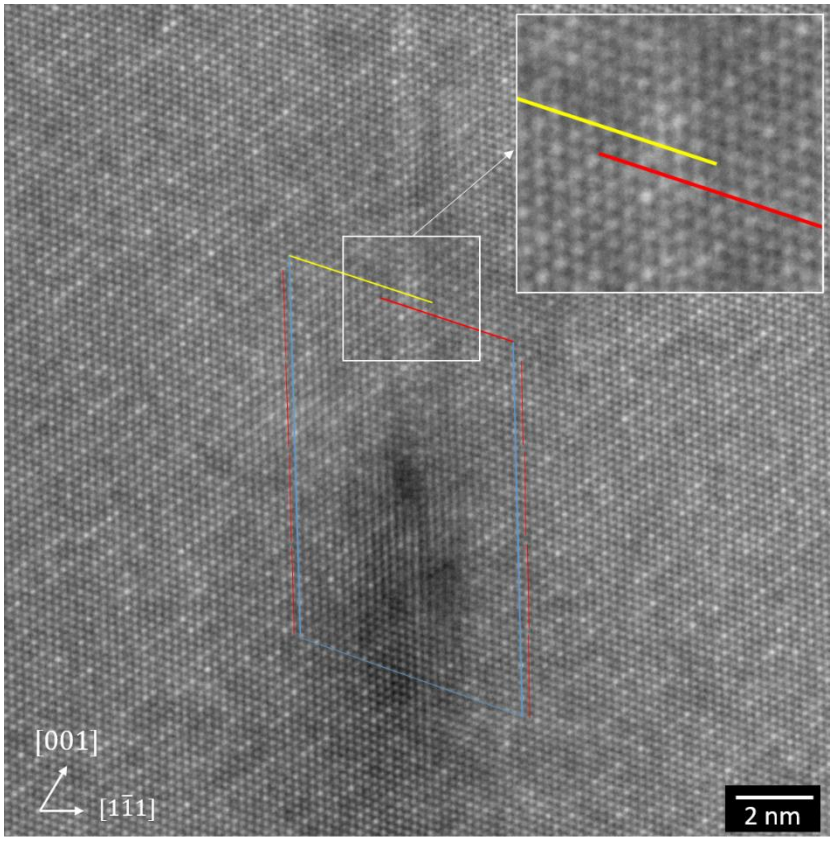

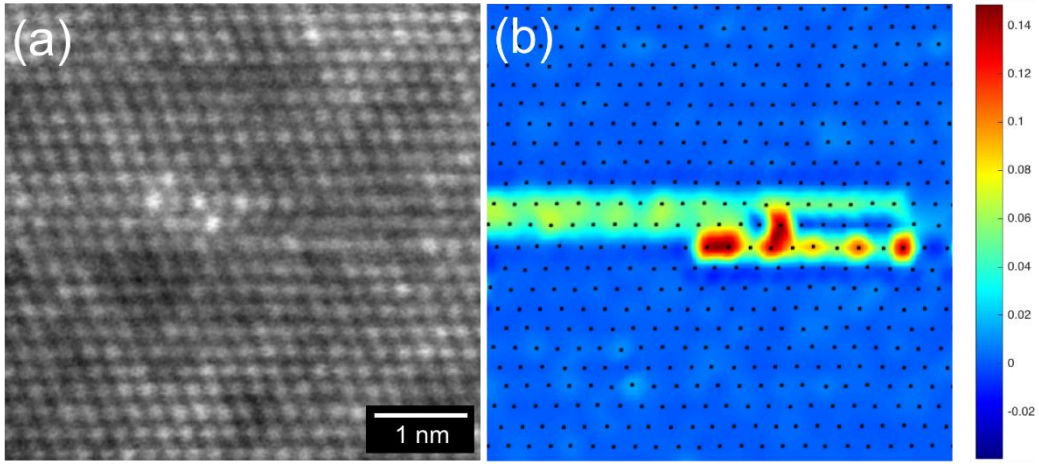

Y. Rao *et al. Acta Mater.*, 2018, vol. 148, pp. 173-184

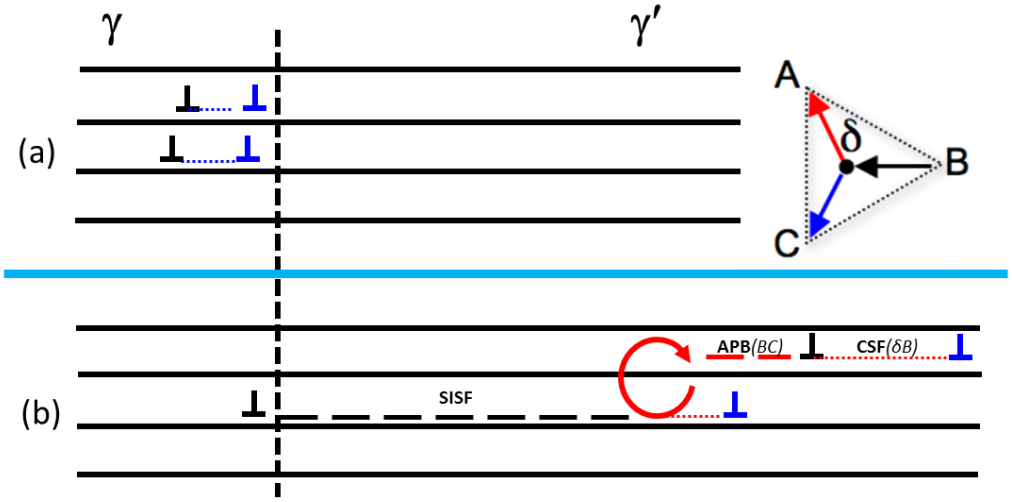

[2]V.A. Vorontsov, *et al. Acta Mater.*, 2012, vol. 60, pp. 4866–78.

- Two like-sign a/2<110>'s interact at the γ/γ´ interface to create an APB and CSF
- The APB and CSF reorders to form low energy SISF – eliminating wrong nearest neighbor bonds

Segregation Along SISFs in CMSX-4

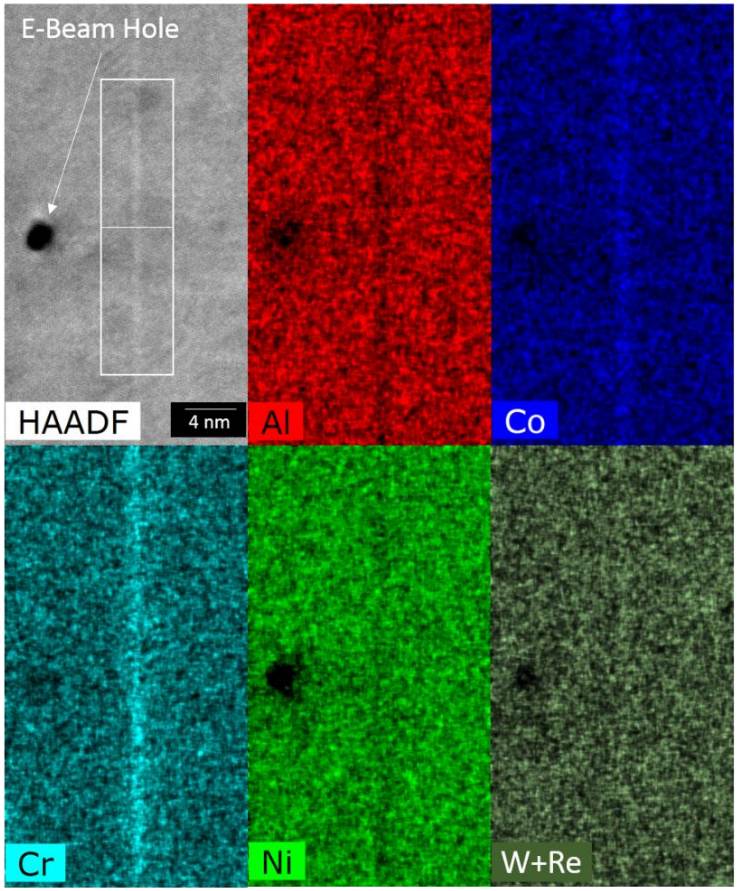

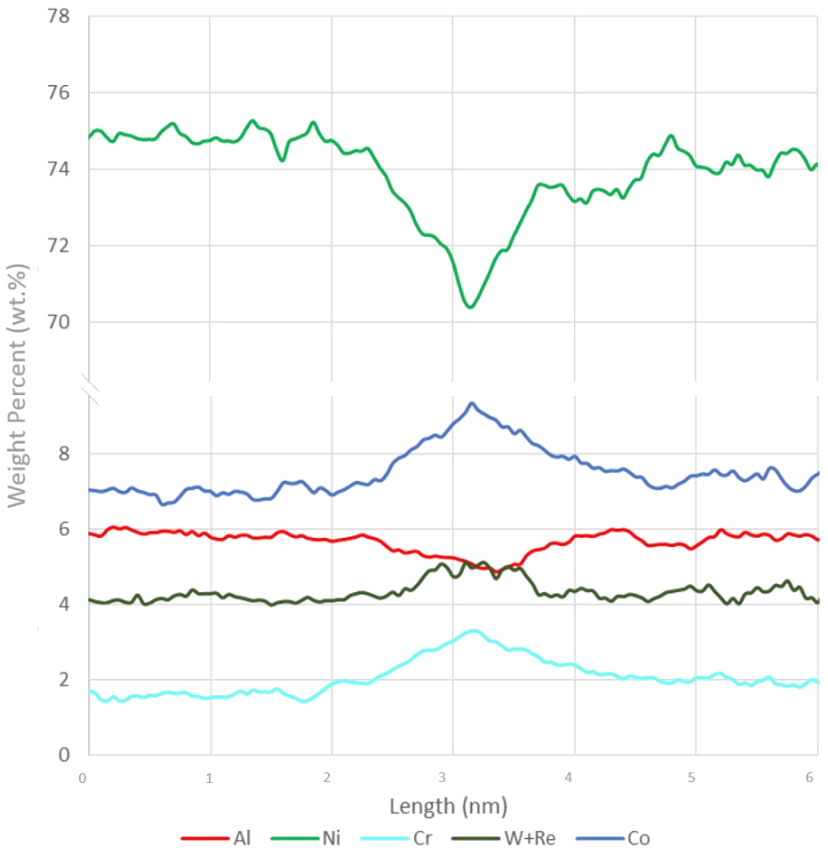

Near atomic resolution EDS mapping found Cr, Co, and W/Re segregation along the SISF, Whereas Ni and Al were depleted.

Segregation Along SISFs in CMSX-4

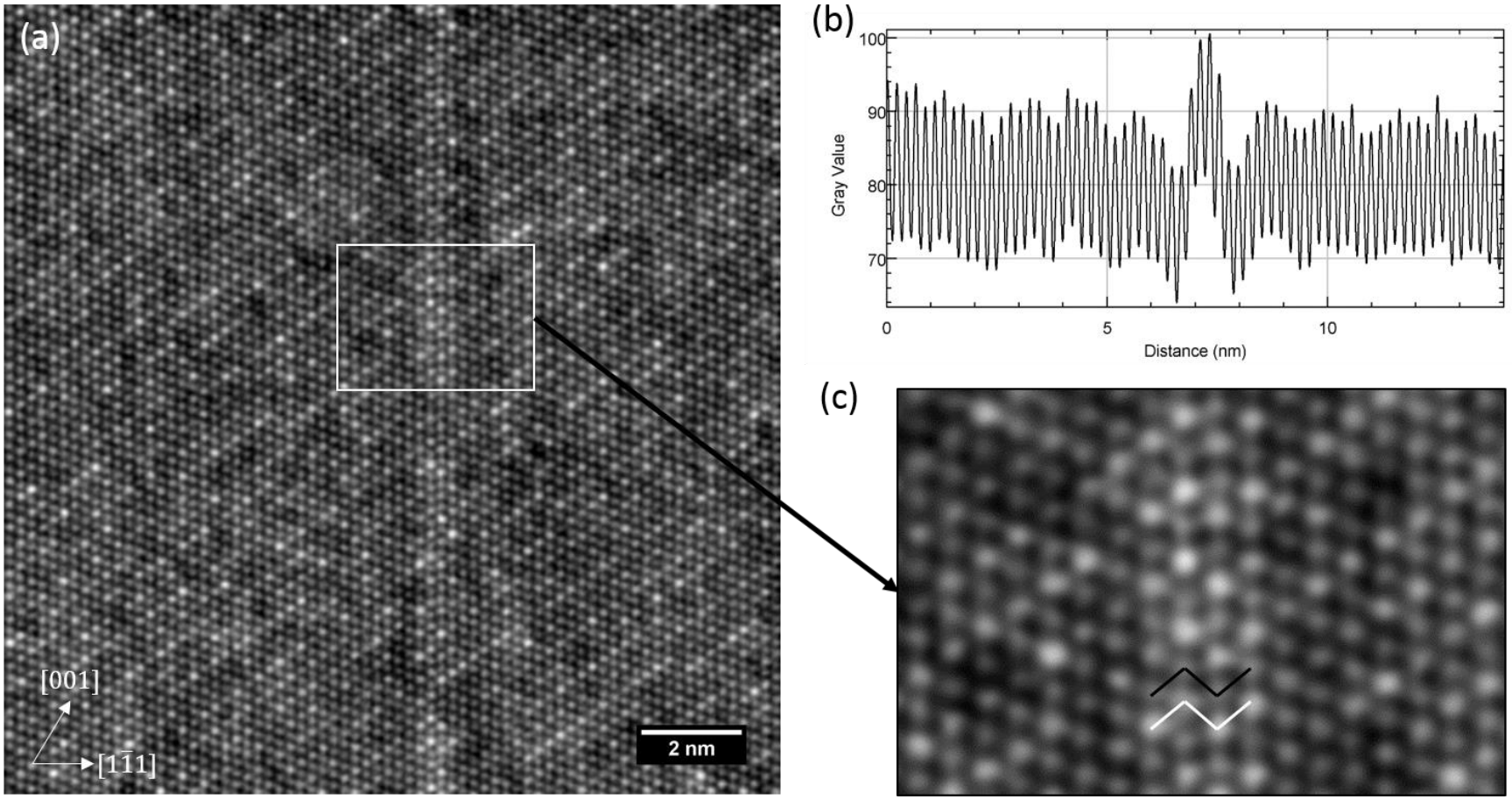

- Ordered contrast along the SISF in CMSX-4
- Muted contrast of the γ' adjacent to the SISF

$D0_{19}$ Phase Transformation Along SISFs in CMSX-4

Co-based Superalloy

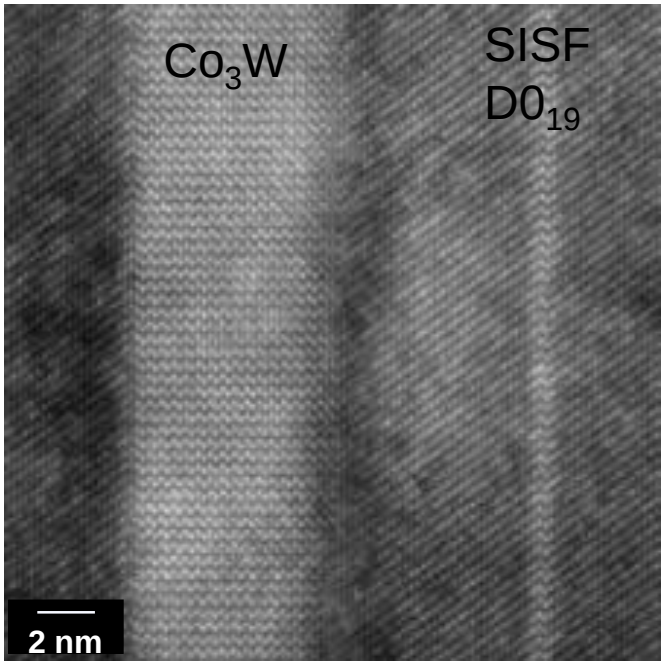

Titus *et al.* Sci. Adv. 2016

Element	γ'	SISF	% Change
Aluminum	5.93 ± 0.2	5.19 ± 0.2	-12.4
Titanium	1.34 ± 0.1	1.41 ± 0.1	5.1
Chromium	**1.95 ± 0.1**	**3.42 ± 0.1**	**75.2**
Cobalt	**4.65 ± 0.3**	**5.76 ± 0.6**	**23.9**
Nickel	76.43 ± 2.2	73.71 ± 2.3	-3.56
Molybdenum	0.32 ± 0.1	0.28 ± 0.1	-10.69
Tantalum	5.18 ± 1.1	5.08 ± 1.0	-1.75
Tungsten + Rhenium	**4.21± 0.7**	**5.13 ± 0.8**	**21.9**

Segregate: Co, Cr, W/Re
Depletion: Ni, Al

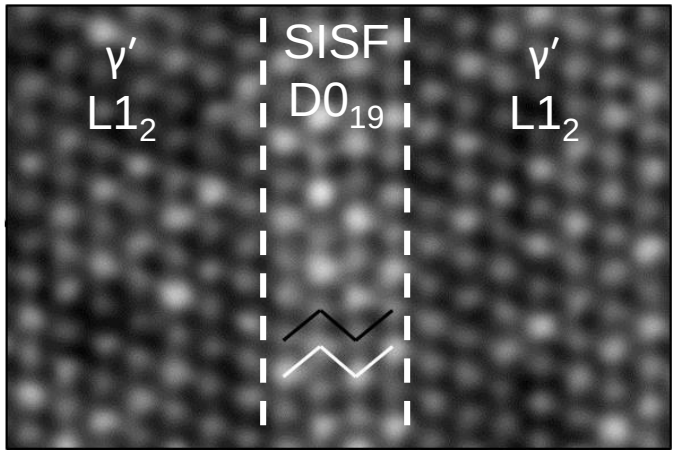

Note: Co_3Cr and Co_3Mo both utilize an ordered HCP $D0_{19}$ crystal structure

Co_3W has a HCP $D0_{19}$ crystal structure – The same found locally along a SISF.

Note: similar ordering contrast and chemistry suggests a γ' → $D0_{19}$ phase transformation along SISFs

$D0_{19}$ Phase Transformation Along SISFs in CMSX-4

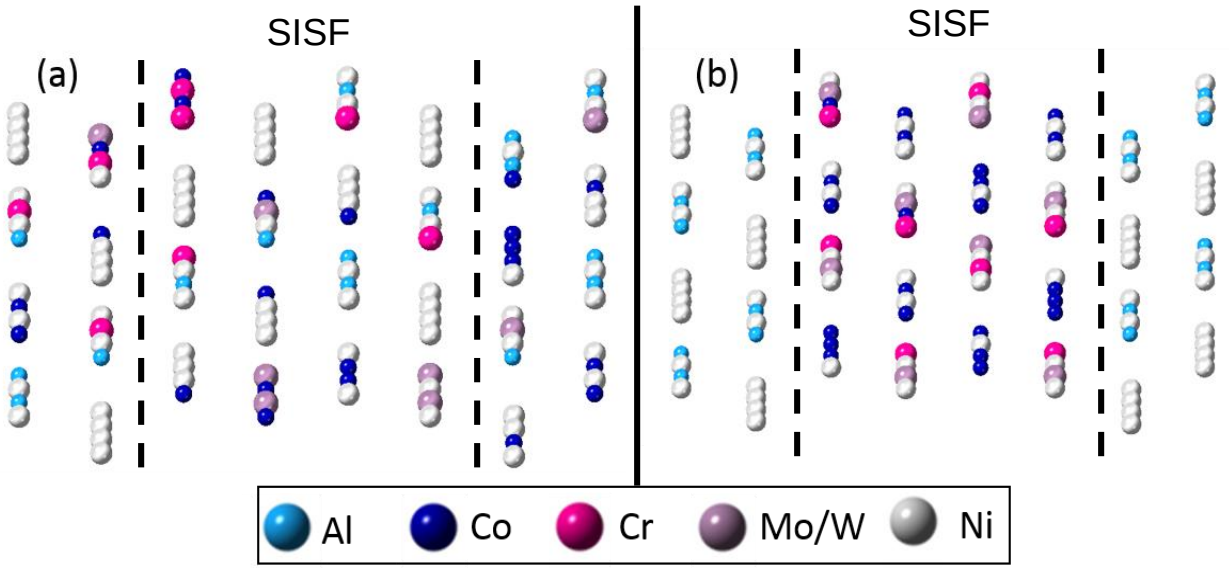

$D0_{19}$ formers Co, Cr, Mo, and W prefer segregating and nucleating the ordered $D0_{19}$ phase along a SISF rather than sitting at random sites throughout the γ' precipitate

$D0_{19}$ Phase transformation	Composition	Random Structure Energy (eV)	Segregated Structure Energy (eV)	Difference (eV)
Co_3(Cr, Mo)	74Ni-22Co-16Al-8Cr-8Mo	-810.07	-812.08	**-2.01eV**
Co_3(Cr, W)	74Ni-22Co-16Al-8Cr-8W	-827.45	-829.49	**-2.04ev**

$D0_{19}$ Phase Transformation Along SISFs in CMSX-4

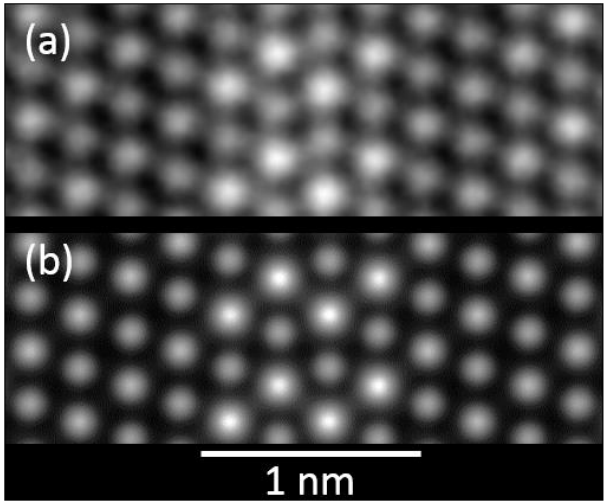

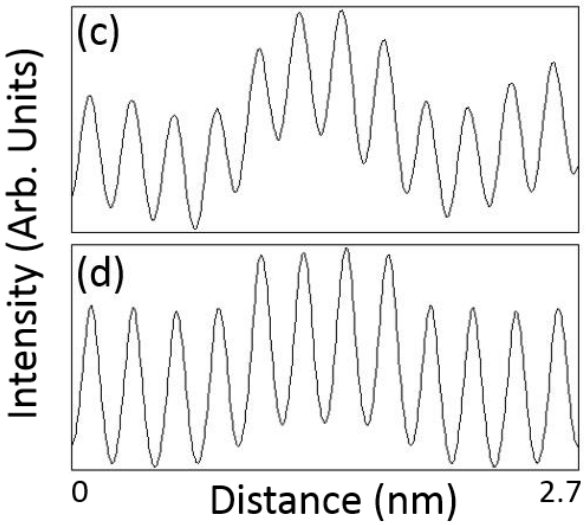

HAADF image consistent with an ordered $D0_{19}$ phase along SISF

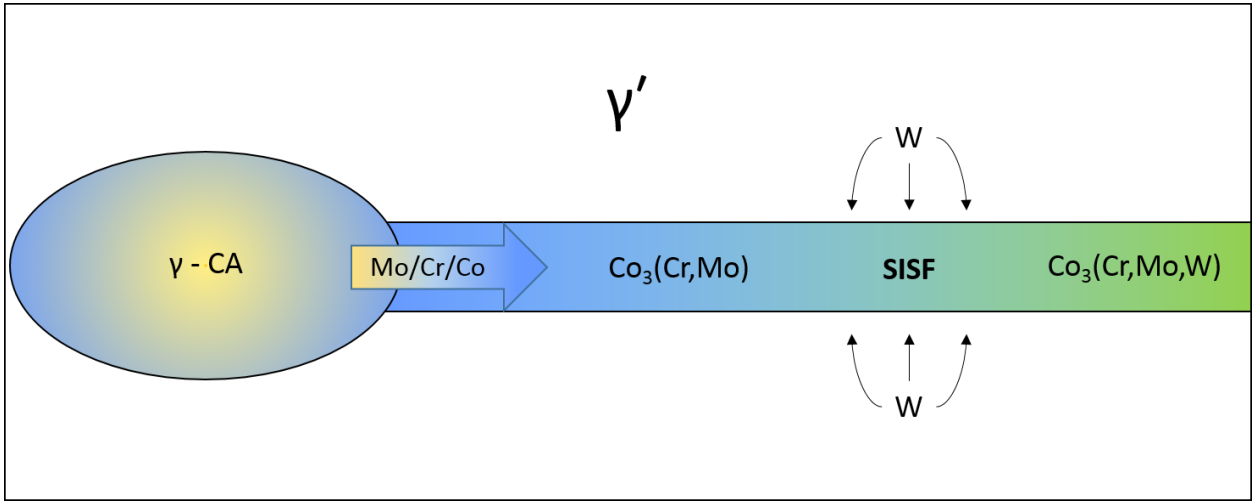

Formation of the $D0_{19}$ phase along SISFs in CMSX-4

Segregation along stacking faults in ME501

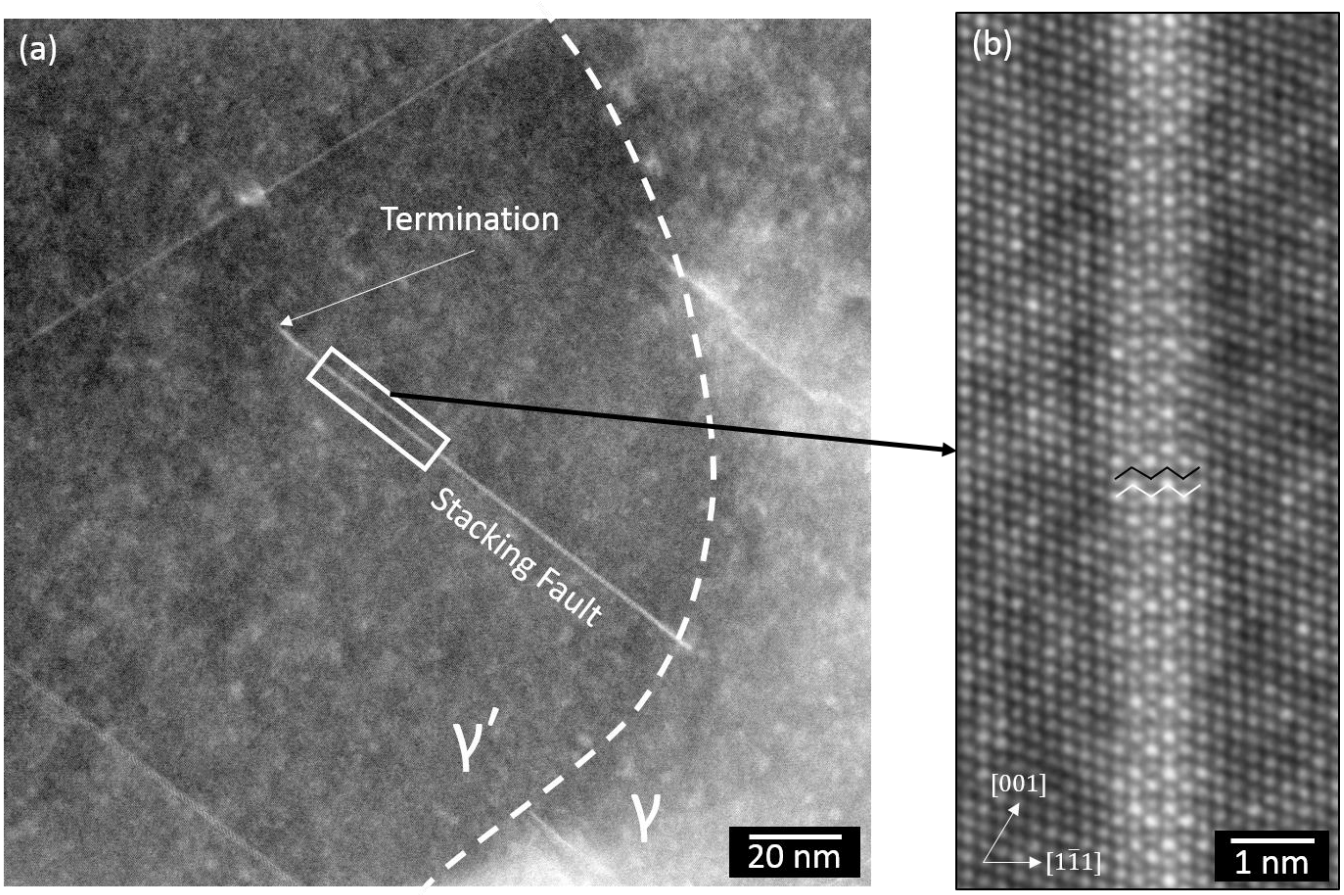

Same ordered contrast observed along the SISF in CMSX-4 is present along the SSF in ME501

Segregation along stacking faults in ME501

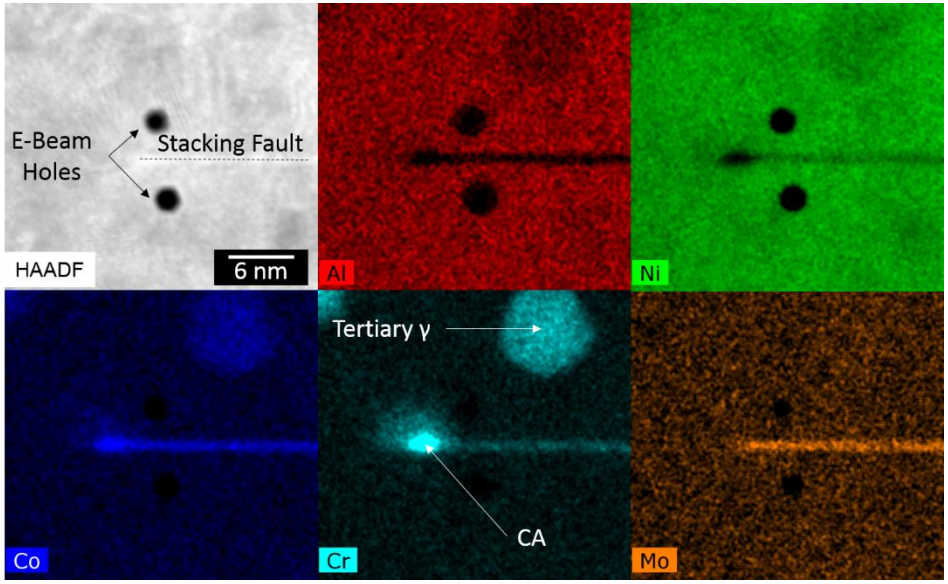

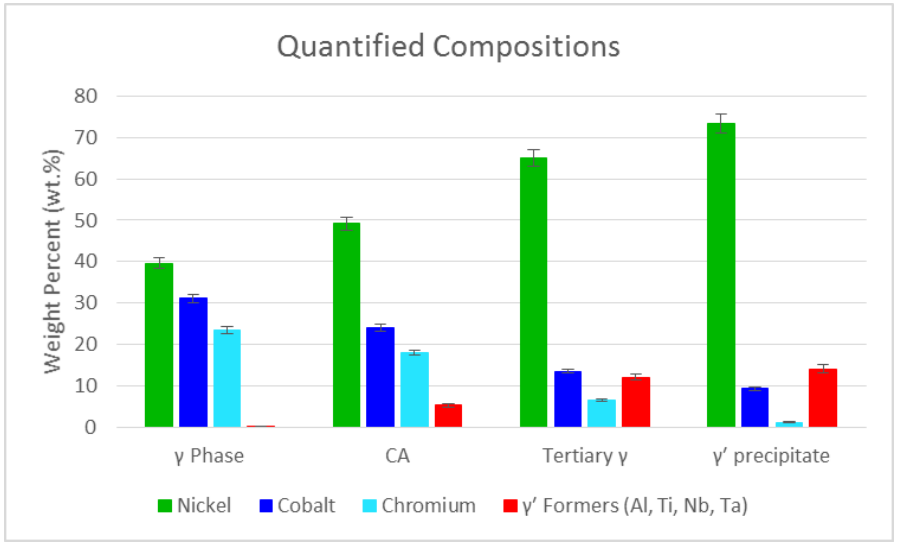

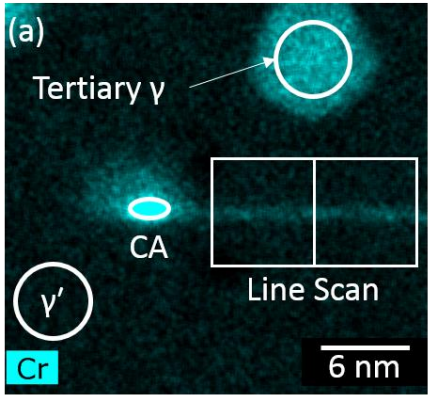

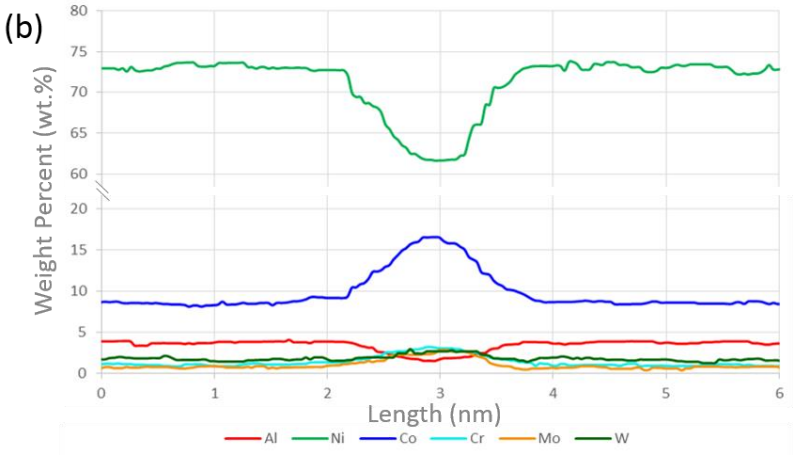

- Near atomic resolution EDS mapping found Cr, Co, and Mo segregation along the SSF, Whereas Ni and Al were depleted.
- A prominent Co/Cr rich Cottrell atmosphere was observed leading the fault.

Double SISF formation in ME501

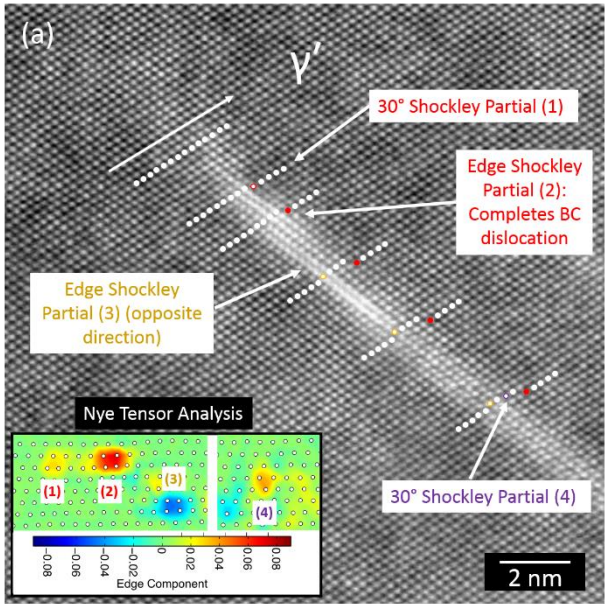

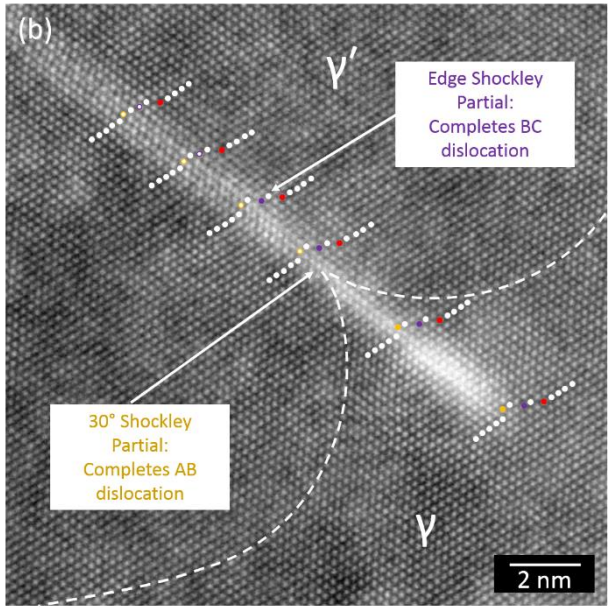

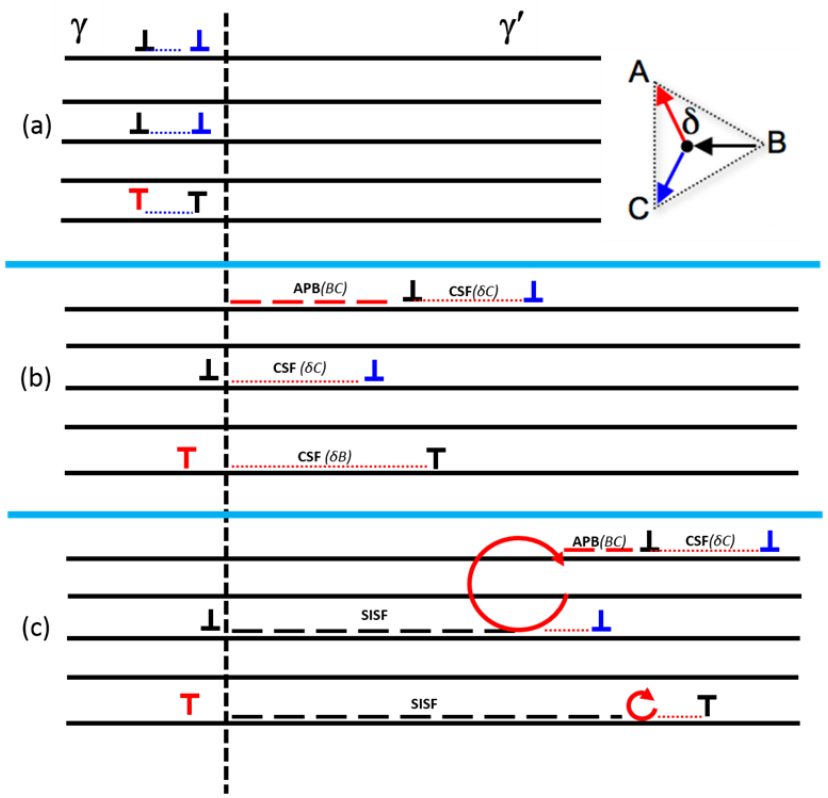

The Double-SISF structure has the same D019 local crystal structure

- **Two of the same dislocation types (CB) and one of opposite sign (BA) each separated by a single {111} layer become pinned at the γ/γ′ interface.**
- **The top dislocation is able to completely enter the precipitate forming an APB behind it and CSF between the two partials. Leading partials from the other two dislocations enter the precipitate forming CSFs of opposite direction burgers vectors behind them.**
- **Through reordering and climb of the partials responsible for the high energy APB the two CSFs can rearrange to form lower energy SISFs.**

$D0_{19}$ Phase Transformation in CMSX-4 and ME501

Alloy	Ni	Cr	Co	Mo	W	Nb	Ta	Al	Ti	Hf	Re	Zr	B	C
ME501	Bal.	12	18	2.9	3	1.5	4.8	3	3	0.4	0	0.05	0.03	0.05
CMSX-4	Bal.	6.5	9.6	0.6	6.4	0	6.5	5.6	1	0.1	3	0	0	0

$D0_{19}$ Phase transformation	**Composition**	**Random Structure Energy (eV)**	**Segregated Structure Energy (eV)**	**Difference (eV)**
Co_3(Cr, Mo)	74Ni-22Co-16Al-8Cr-8Mo	-810.07	-812.08	**-2.01eV**
Co_3(Cr, W)	74Ni-22Co-16Al-8Cr-8W	-827.45	-829.49	**-2.04ev**

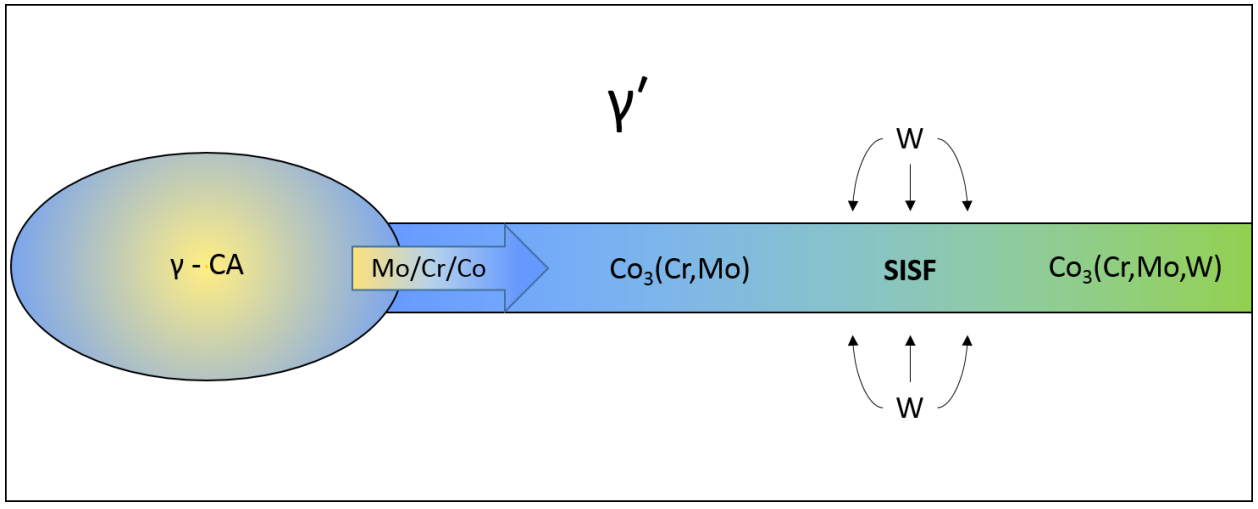

The amount of Mo and W segregation along the SISF appears directly related to the amount present in the bulk alloy.

Conclusions

- High resolution HAADF-STEM imaging and EDS analysis found an ordered segregation of Co, Cr, Mo and W and a depletion of Ni and Al along SISFs in two different Ni-base superalloys.
- The dislocation structure responsible for the 2-SISF configuration observed in ME501 presents a new, more complex reordering process than has been previously reported and exposes multiple pathways with which SISFs can form. This includes the possibility of different dislocations separated by only a single atomic plane at the γ/γ' interface.
- DFT VASP calculations and HAADF-STEM image simulations validate the existence of an ordered hexagonal $D0_{19}$ Co_3(Cr, Mo, W) phase nucleated along SISFs in both Ni-base superalloys.
- A prominent Cr and Co rich Cottrell atmosphere exists around shearing Shockley partials which is likely the rate limiting feature during γ' shearing
- Diffusion mediated segregation processes must be incorporated in physics-based modeling of creep and dwell fatigue at intermediate temperatures
- **Alloy design is alive and aided by advanced characterization and modeling**

Acknowledgments

Questions?

- CEMAS (OSU)
- GE Aviation
- Bob Carter
- Tim Gabb
- Cheryl Bowman
- Steve Arnold
- Jack Telesman
- Laura Evans
- Pete Bonacuse
- Dave Ellis
- Joy Buehler